



# Hydrothermal alteration and fluid pH in alkaline-hosted epithermal systems



Daniel J. Smith<sup>a,\*</sup>, Jonathan Naden<sup>b</sup>, Gawen R.T. Jenkin<sup>a</sup>, Manuel Keith<sup>a</sup>

<sup>a</sup>Department of Geology, University of Leicester, UK

<sup>b</sup>British Geological Survey, Keyworth, Nottingham NG12 5GG, UK

## ARTICLE INFO

### Article history:

Received 6 April 2017

Received in revised form 14 June 2017

Accepted 30 June 2017

Available online 1 July 2017

## ABSTRACT

Epithermal gold mineralisation is found in a wide compositional range of host lithologies, but despite the diversity the alteration mineral assemblages are often similar between deposits. Notable exceptions are those gold deposits hosted in alkaline host rocks. Alkaline-hosted epithermal deposits are rare, but important, as they include some of the world's largest known epithermal deposits by contained metal (e.g. Ladolam, Cripple Creek, Porgera). As well as the exceptional gold contents, the alkaline-hosted systems tend to exhibit different alteration mineral assemblages, with less quartz and widespread silicification than sub-alkaline-hosted equivalents, and greater enrichments in tellurium, and a scarcity of acid alteration (advanced argillic) types. In this study, geochemical modelling is used to demonstrate that 300 °C hydrothermal fluids in equilibrium with alkali, silica-undersaturated host rocks at low water/rock ratios reach significantly higher pH than equivalents in sub-alkaline lithologies. A maximum, near-neutral pH (5.5–6) is buffered by reactions involving quartz in silica-saturated alkaline and calc-alkaline lithologies. In silica-undersaturated, alkaline host rocks, quartz is exhausted by progressive water-rock interaction, and pH increases to 7 and above. Both tellurium and gold solubility are favoured by neutral to high fluid pH, and thus there is a clear mechanism within these hydrothermal systems that can lead to effective transport and concentration to produce gold telluride ore deposits in alkaline igneous hosts. This modelling demonstrates that alkaline rocks can still be altered to advanced argillic assemblages; the paucity of this alteration type in alkaline hosts instead points to NaCl ≫ HCl in magmatic volatile phases at the initiation of hydrothermal alteration.

© 2017 The Authors. Published by Elsevier B.V. This is an open access article under the CC BY license (<http://creativecommons.org/licenses/by/4.0/>).

## 1. Introduction

Epithermal Au (Ag) deposits form in shallow hydrothermal and magmatic-hydrothermal systems. A number of studies (Richards, 1995; Jensen and Barton, 2000; Müller, 2002; Sillitoe, 2002) have recognised that epithermal deposits developed in alkaline host rocks tend to have anomalous features relative to calc-alkaline hosted systems – they are commonly gold- and telluride-rich, have less hydrothermal quartz, and limited development of acidic (sericitic and advanced argillic) alteration styles (Jensen and Barton, 2000). Of particular note is the recognition that the alkaline-associated deposits tend to be well endowed with gold – indeed, the world's largest epithermal Au deposit is hosted in alkaline rocks (Ladolam, Lihir Island, Papua New Guinea; Simmons and Brown, 2006). The alkaline-hosted epithermal deposits are enriched in a range of “critical” elements in addition to Te, including platinum group elements (PGE), F, W, and V (Kelley and Spry,

2016). The successful exploration and exploitation of these deposits depends on a robust model of their alteration zonation and geochemistry (i.e. pathfinder enrichments and anomalies).

Epithermal Au deposits are most commonly hosted in sub-alkaline basaltic to rhyolitic rocks (Fig. 1; du Bray, 2017). An important study by Reed (1997) modelled water-rock reaction in such a range of host rocks, and showed that the alteration assemblages and water chemistry progressed through a repeatable set of compositions (for a given temperature and starting fluid) with minimal variation between the different hosts. Epithermal deposits are consequently considered in terms of the starting fluid chemistry and degree of equilibration with the host, with much less emphasis placed on the composition of the host. Epithermal Au deposits are often subdivided (e.g. Heald et al., 1987; Hedenquist et al., 2000) into: “high sulphidation”, “acid sulphate” or “quartz-alunite” type, dominated by intensely leached “advanced argillic” alteration, with magmatic-derived Cl<sup>-</sup> and SO<sub>4</sub><sup>2-</sup>-rich acidic fluids driving this alteration; and “low sulphidation”, “adularia-sericite” or “quartz-adularia” type, with alkali-bearing alteration assemblages, produced by rock-buffered, near-neutral chloride fluids.

\* Corresponding author.

E-mail address: [djs40@le.ac.uk](mailto:djs40@le.ac.uk) (D.J. Smith).

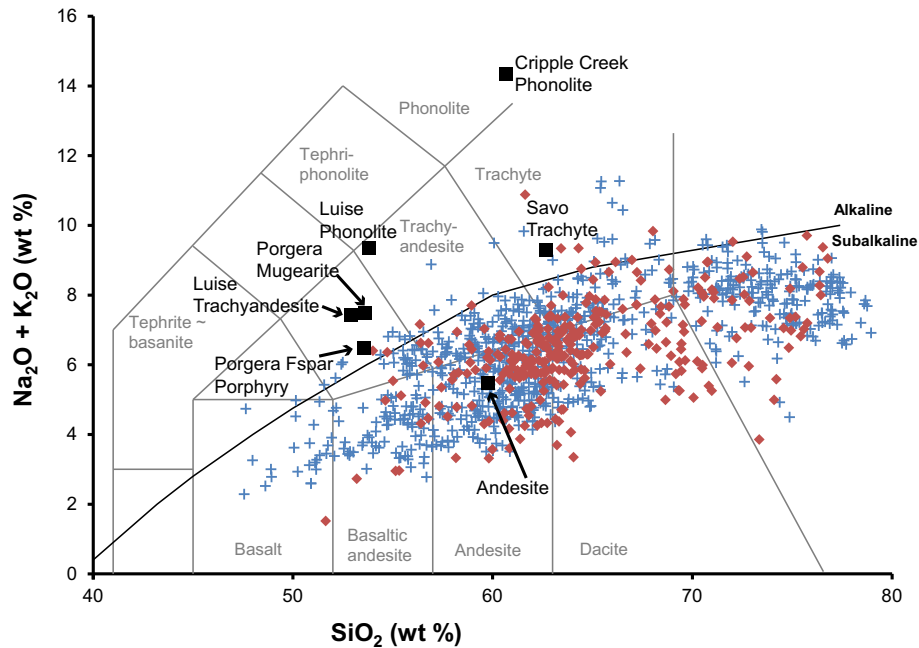


**Fig. 1.** Total alkali vs silica plot showing compositional range of typical host rocks for high sulphidation (red circles) and low sulphidation epithermal deposits (blue crosses) from Du Bray (2014, 2017). Black boxes show the alkaline host rock compositions used for models in this study (Table 1). Black curve represents the alkaline/sub-alkaline boundary of Irvine and Baragar (1971).

The alkaline-hosted systems are typically considered a sub-class of the low sulphidation deposits (Richards, 1995; Jensen and Barton, 2000; Kelley and Spry, 2016), given the similarity in alteration assemblages; however, the notable differences listed in the previous paragraph mark them out as distinct.

In this study, we explore the consequences of host rock composition on deposit mineralogy and fluid chemistry. Considering the host rock as the only variable represents a gross simplification of the complexity within the range of epithermal deposits and their formative hydrothermal systems. However, we will demonstrate that in the alkaline-hosted systems, the host composition alone can account for a number of the distinctive features of the final deposits.

## 2. Host rock composition and alteration assemblages

Reed (1997) modelled the progressive water-rock reaction at 300 °C between initially acidic, condensed magmatic vapour with basalt, andesite and dacite, representing the common range of host compositions for epithermal Au deposits (du Bray, 2017). Titration of the rock into the initial fluid results in a progressive increase in the fluid pH (Fig. 2a), and precipitation of minerals (Fig. 2c). pH increase is often in a flat-step morphology as it is buffered by the alteration mineral assemblage (Reed, 1997). The mineral assemblages (Fig. 2e) progress from advanced argillic (quartz + alunite + pyrophyllite) through sericite-chlorite (quartz + muscovite/sericite + paragonite + chlorite) to propylitic (quartz + epidote + chlorite + alkali feldspar). This progressive change in mineralogy mirrors the zonation of alteration from the core to periphery of a high sulphidation type system (Arribas, 1995). The progressive titration can be considered in terms of decreasing water-rock ratio ( $w/r$ ). High sulphidation deposits exhibit alteration assemblages consistent with volcanic gas-rich, high  $w/r$  conditions (i.e. fluid-buffered), whereas low sulphidation deposits exhibit alteration assemblages consistent with low  $w/r$  values (Giggenbach, 1997).

The modelling does not imply that all epithermal deposits were produced from neutralisation of an initially acidic fluid. Hydrothermal fluids may be derived from relatively well-equilibrated

(i.e. apparently low  $w/r$ ) waters that shift to progressively high  $w/r$  in zones of focussed fluid flow. On figures with an x-axis of  $w/r$ , progress can be read from right-to-left as well as left-to-right.

## 3. Methods

The progressive water-rock reaction between 1 kg of initially acidic, condensed magmatic vapour and a series of different rock compositions was modelled with CHILLER (Reed, 1982, 1998), and follows the design of the water-rock reactions of Reed (1997). The thermodynamic data used in the numerical experiments are from the database SOLTHERM.H08 (Reed and Palandri, 2013). Data and calculations within SOLTHERM include: equilibrium constants calculated with SUPCRT92 (Johnson et al., 1992); mineral thermodynamic data for silicates, oxides, hydroxides, carbonates, gases (Holland and Powell, 1998) and sulphides (Shock, 2007). Mineral solid solutions are represented by end-member compositions that are mixed using an ideal multisite mixing scheme.

Rock compositions used in the modelling represent a sub-alkaline andesitic control, and a number of alkaline compositions associated with world-class Au deposits, summarised in Table 1. The analyses used were those representing least-altered igneous compositions that most closely resemble the pre-hydrothermal litho-geochemistry; we have not modelled complex spatial heterogeneity or the full range of compositions reported from each deposit area, as the purpose of these models is to show first-order effects of host rock composition, not produce detailed reconstructions of the alteration zonation of each system.

All starting rock compositions are derived from whole rock geochemical data, and have been recalculated to a 100% basis without  $TiO_2$  or  $P_2O_5$  (excluded as minor phases with little to no effect on hydrothermal mineral assemblages). Original total Fe (as  $Fe_2O_3$ ) has been recalculated to FeO and  $Fe_2O_3$  using the method of Müller et al. (2001). Silica saturation index is calculated on the basis of CIPW-normative mineralogical composition, using the equation

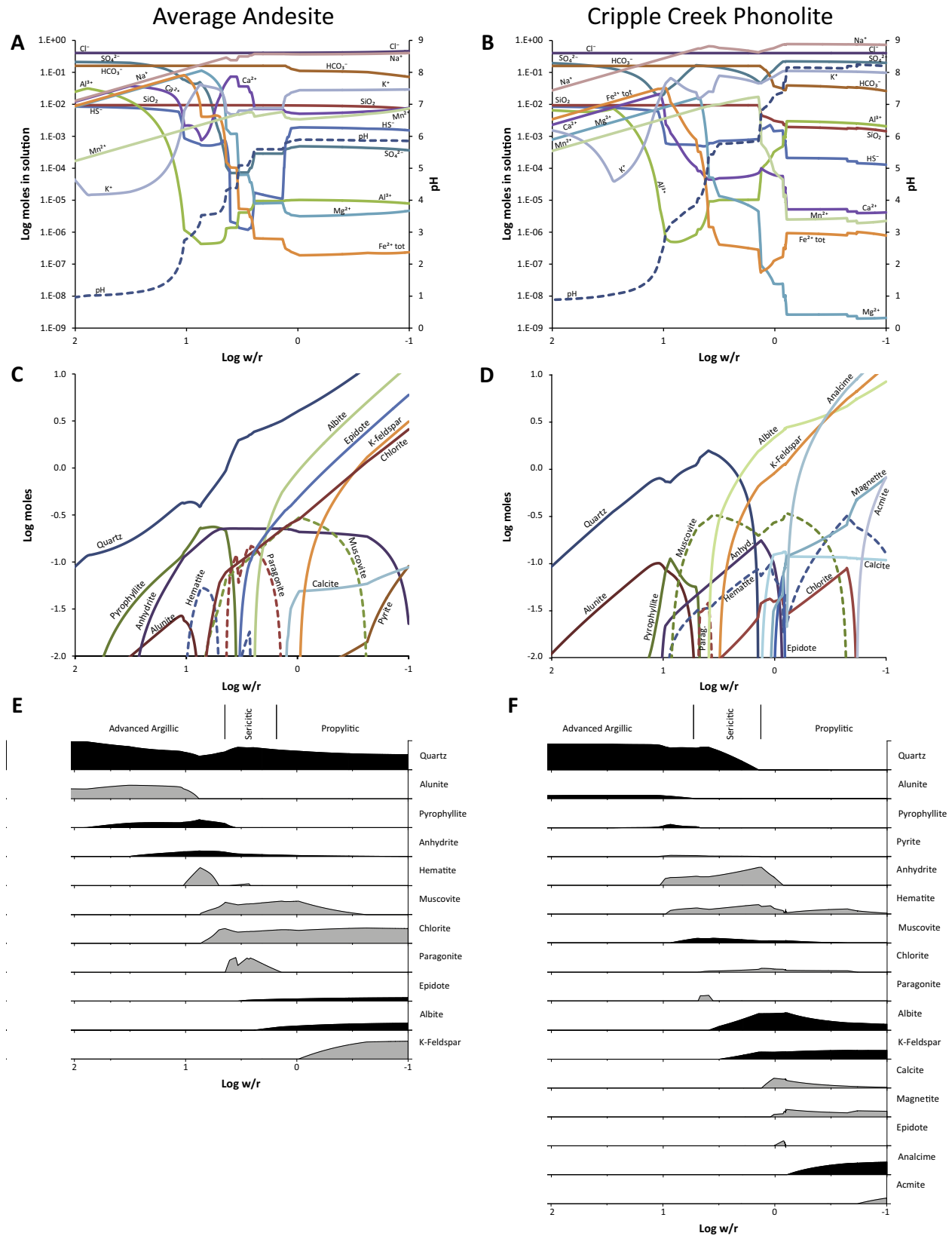


**Fig. 2.** Modelled titration of Average Andesite and Cripple Creek Phonolite into initially acidic hydrothermal fluid at 300 °C (after Reed, 1997). Reaction progress is from left to right in high sulphidation-type environments; in low sulphidation environments with lower direct input of magmatic volatiles progress is right-to-left with increased flux through veins. a and b) Hydrothermal fluid composition after titration with andesite and phonolite. c and d) Minerals produced from titration with andesite and phonolite, displayed as log moles present in solids. e and f) Mineral assemblages from titration of andesite and phonolite, displayed as % of solids. Minerals in black are shown on axes that range 0–100%; those in grey have axes with range 0–10%. Minerals with maximum abundance <1% are not shown.

**Table 1**

Summary geochemical data for igneous rock compositions used in models.

Reference Sample #	Andesite (Reed, 1997)	Savo Sodic Trachyte (Smith et al., 2009) SV40	Porgera Feldspar Porphyry (Richards, 1990) RJR-56	Porgera Mugearite (Richards, 1990) RJR-09	Luise Trachyandesite (Müller et al., 2001) 20	Luise Phonolite (Müller et al., 2001) 22	Cripple Creek Phonolite (Kelley et al., 1998) CC004
SiO <sub>2</sub>	59.07	62.90	53.95	53.38	54.18	54.24	60.87
Al <sub>2</sub> O <sub>3</sub>	17.43	17.90	17.70	19.17	19.34	19.36	20.19
Fe <sub>2</sub> O <sub>3</sub>	2.56	1.25	3.43	4.15	7.68	5.85	1.99
FeO	4.05	2.49	3.84	3.22	1.22	0.93	0.67
MnO	0.12	0.09	0.18	0.18	0.22	0.20	0.25
MgO	3.35	2.10	5.14	3.54	2.50	2.60	0.32
CaO	6.77	3.78	9.04	8.79	7.25	7.31	1.29
Na <sub>2</sub> O	3.93	7.01	4.72	5.61	3.76	4.77	8.51
K <sub>2</sub> O	1.48	2.32	1.80	1.87	3.81	4.65	5.89
BaO	0.07	0.09	0.04	0.06	0.04	0.09	0.04
S native	0.02	0.04	0.16	0.02			
CuO <sub>0.5</sub>	0.01	0.003	0.008	0.008	0.009	0.02	0.0005
PbO	0.0008	0.002	0.0001	0.0005			0.003
ZnO	0.01	0.005	0.01	0.01	0.006	0.009	0.02
hy	10.66	2.77	0.00	0.00	1.99	0.00	0.00
q	10.30	4.14	0.00	0.00	0.00	0.00	0.00
ne	0.00	0.00	1.10	5.64	0.00	6.96	14.54
di	6.56	5.23	16.15	14.77	7.09	12.24	1.67
SSI	0.89	0.79	-0.06	-0.28	0.22	-0.36	-0.90

All data in wt% except SSI. Data recalculated to 100 wt% on an anhydrous, TiO<sub>2</sub> and P<sub>2</sub>O<sub>5</sub>-free basis. FeO/Fe<sub>2</sub>O<sub>3</sub> recalculated from original FeO<sup>TOTAL</sup> using the method of (Müller et al., 2001). Hy = normative hypersthene; q = normative quartz; ne = normative nepheline; di = normative diopside; SSI = silica saturation index, calculated with Eq. (1).

$$SSI = \frac{\text{Hypersthene} + 4 \text{ Quartz} - \text{Nepheline}}{\text{Hypersthene} + \text{Diopside} + 4 \text{ Quartz} + \text{Nepheline}} \quad (1)$$

Silica-saturated, hypersthene- and quartz-normative compositions have positive SSI values. Silica-undersaturated, nepheline-normative compositions have negative SSI values.

The andesite is representative of calc-alkaline, silica saturated compositions, and is derived from and discussed in detail in Reed (1997). The Luise “Phonolite” (a trachyandesite using the Le Maitre et al., 1989 TAS plot; Fig. 1) and Trachyandesite are from the vicinity of the Ladolam epithermal Au deposit, Lihir Island, Papua New Guinea (Müller et al., 2001). The Porgera Mugearite and Feldspar Porphyry represent unaltered host rock compositions (Richards, 1990) from the Porgera Au deposit (Papua New Guinea). The Cripple Creek Phonolite is part of the host suite to the Cripple Creek epithermal Au deposit, Colorado (Kelley et al., 1998). The Savo trachyte (Smith et al., 2009) represents a typical host rock of the active hydrothermal system (Smith et al., 2010), on Savo island, Solomon Islands. With the exception of the Andesite, all compositions are alkaline using the total alkali versus silica definition of Irvine and Baragar (1971). The Savo sample is not associated with known epithermal Au mineralisation; this composition was selected on the grounds that it represents an evolved (SiO<sub>2</sub>-rich) silica-saturated, alkaline composition.

The initial fluid composition is based on a condensate from Augustine volcano (Symonds et al., 1990) mixed 1:10 with pure water (Reed, 1997; Table 2). A single starting fluid for all models was chosen so as to demonstrate the effect of host rock alone. The condensate acts as a source for anions (Cl<sup>-</sup>, SO<sub>4</sub><sup>2-</sup>, HCO<sub>3</sub><sup>-</sup>) for the models. At low w/r the chemistry of the fluid is largely controlled by host rock composition so initial starting fluid has relatively little influence on late mineral assemblages and fluid compositions.

All model runs were carried out at 300 °C and at the pressure vapour-liquid saturation in water. The chosen temperature reflects the upper conditions typical of low sulphidation epithermal mineralisation (Simmons et al., 2005), but appropriate for initial conditions of fluids in high sulphidation systems, and for alkaline-hosted low sulphidation systems presuming a significant magmatic fluid input.

**Table 2**

Initial fluid composition used in models.

Species	Molality	mg kg <sup>-1</sup>
Cl <sup>-</sup>	0.40	13656
SO <sub>4</sub> <sup>2-</sup>	0.22	19924
HCO <sub>3</sub> <sup>-</sup>	0.16	9331
HS <sup>-</sup>	8.85 × 10 <sup>-3</sup>	280
SiO <sub>2</sub> (aq)	5.45 × 10 <sup>-4</sup>	31.3
Al <sup>3+</sup>	1.77 × 10 <sup>-6</sup>	0.0456
Ca <sup>2+</sup>	3.02 × 10 <sup>-6</sup>	0.116
Mg <sup>2+</sup>	3.15 × 10 <sup>-7</sup>	0.00732
Fe <sup>2+</sup>	1.05 × 10 <sup>-5</sup>	0.560
K <sup>+</sup>	5.71 × 10 <sup>-5</sup>	2.13
Na <sup>+</sup>	9.20 × 10 <sup>-5</sup>	2.02
Mn <sup>2+</sup>	1.12 × 10 <sup>-7</sup>	0.00588
Zn <sup>2+</sup>	4.20 × 10 <sup>-6</sup>	0.262
Cu <sup>+</sup>	4.53 × 10 <sup>-7</sup>	0.0275
Pb <sup>2+</sup>	1.58 × 10 <sup>-6</sup>	0.313
Ba <sup>2+</sup>	1.84 × 10 <sup>-9</sup>	2.42 × 10 <sup>-4</sup>
pH @ 300 °C	0.79	

Composition is that of Reed (1997), derived from fumarole condensate from Augustine volcano (Symonds et al., 1990) in 10 parts pure water.

Specified compositions of rocks are titrated into the fluid; progressive titrations are recorded by decreasing w/r. The model is closed and precipitating minerals are retained for possible back-reactions. Titration increment sizes were reduced for intervals of complexity (multiple minerals saturating or under-saturating) to avoid the iterative calculations failing. A low log (w/r) value of -1.0 was selected as the end point for the modelled titrations (modelled as 10,000 g rock incrementally added to 1000 g initial fluid). At log (w/r) less than -1.0, significant water is consumed by the formation of hydrous silicate minerals and “dry up” of the system occurs (Reed, 1997).

#### 4. Results

All modelled titrations start from a common fluid composition with pH 0.8. Progressive addition of rock to the fluid (i.e. decreasing w/r) causes an increase in pH with a flat-step morphology (Fig. 3). Silica-saturated compositions (Average Andesite, Savo trachyte and Luise Trachyandesite) have relatively little change



The abundance of albite in the fresh and altered mineral assemblage, and the high concentration of  $\text{Na}^+$  in the aqueous solution means that this equilibrium has sufficient capacity to maintain pH until “dry up”.

In silica-undersaturated hosts, the signature of equilibrium fluids under low w/r conditions is a quartz-free alteration assemblage, with key minerals being alkali feldspars, muscovite, epidote group, carbonates, and zeolites (e.g. analcime). Quartz-poor alteration assemblages produced in these models are consistent with the observation that alkaline-hosted Au deposits have less hydrothermal quartz and widespread silicification than calc-alkaline hosted systems (Jensen and Barton, 2000, 2008). Quartz-poor propylitic assemblages are reported as early-stage alteration at both Porgera (Richards and Kerrich, 1993) and Ladolam (Carman, 2003). Acmite and analcime are reported in phonolite intrusion-related alteration at Cripple Creek (Jensen and Barton, 2008).

When quartz is absent from the assemblage, pH is no longer maintained at the propylitic buffer and hydrothermal fluids at low water/rock ratios develop pH values significantly higher than equivalent fluids in silica-saturated hosts (Fig. 4). Although low w/r values suggest that the aqueous phase is much smaller than the rock in terms of mass, many parts of hydrothermal systems and hydrothermal ore deposits are or were low w/r phenomena, as evidenced by volumetrically significant, often regional-scale, propylitic alteration in epithermal and porphyry-Cu (Mo-Au) deposits (Sillitoe, 2010; Simmons et al., 2005). Although subordinate to the rock phase in terms of mass, there is still ample “working fluid” in these parts of the system to alter rocks and transport various elements.

### 5.2. Acidic alteration and initial fluid conditions

Reviews of hydrothermal systems in alkaline rocks (Jensen and Barton, 2000; Sillitoe, 2002) have highlighted the paucity of acidic (advanced argillic) alteration and high sulphidation/acid-sulphate type ore bodies. The models we present do not suggest that fresh alkaline rocks have a greater capacity to neutralise acidity: all modelled systems are sufficiently acidic ( $\text{pH} < 3$ ) under fluid dominant conditions ( $\log w/r < -1$ ) to generate advanced argillic mineral assemblages of quartz + alunite  $\pm$  pyrophyllite (Fig. 3 and Fig. 2d). Silica-undersaturated compositions reach a higher maximum fluid pH, but the initial acidity of the fluid is neutralised by a similar mass of rock irrespective of composition. Thus, if the fluids in a hydrothermal system are acidic, then advanced argillic alteration will be produced even if the hosts are alkaline. Kelley and Spry (2016) commented that although less common and less intensely developed than in sub-alkaline hosted epithermal deposits, acidic alteration is not entirely absent from alkaline-hosted systems. The limited development of intense acidic alteration in alkaline-associated systems may instead be related to the initial magmatic volatile phase; fluids exsolved from a sub-alkaline melt will include a larger HCl component, whereas in fluids from alkaline magmas Cl will be coordinated to alkali and alkali earth metals (Webster et al., 2014) and preferentially retained in aqueous liquids (brines) or as salt melts, rather than partition into a vapour phase. Liquids and brines exsolving from alkaline magmas would be buffered to neutral to alkaline pH by the magma composition (Jensen and Barton, 2000). The lack of acid alteration and acid fluid-related “high sulphidation” ore bodies in alkaline rocks is likely a result of a lower contribution of HCl into the hydrothermal fluid, and consequently higher initial fluid pH and a predominance of rock-buffered fluid compositions. In Fig. 2, the initial fluid would be in equilibrium with a large volume of rock or melt (assuming magmatic  $\text{H}_2\text{O} < 10$  wt%, equivalent to  $\log w/r -0.95$ ), and hence the system would start on the right hand side of the axis and progress left in zones of focussed fluid flux.

### 5.3. Alkaline rocks and ore deposits

High pH hydrothermal fluids are capable of transporting higher concentrations of Te (McPhail, 1995) than near-neutral equivalents. Grundler et al. (2013) produced experimental results for aqueous solutions (0–1 m NaCl) at 200 °C that showed  $\text{TeO}_2$  solubility to be at least one order of magnitude greater at pH 8 than pH 5, and model results showing a similar enhanced Te-solubility at 300 °C under mildly reducing conditions ( $\log f\text{O}_2 = -30$  to  $-35$ ; close to the magnetite-hematite redox buffer). Under similar conditions, gold would be predominantly transported as  $\text{Au}(\text{HS})_2^-$  (Stefánsson and Seward, 2004); at 300 °C gold solubility would be highest at pH above neutral (pH  $\sim 7$ ), albeit with a sharp drop-off at  $\text{pH} > 8$ . Thus, fluids at pH values above neutrality, possible in alkaline host rocks (Fig. 3), would be more effective at transporting Au and Te than near-neutral fluids expected in calc-alkaline, silica saturated systems. In host rocks with a very low silica saturation index (e.g. the Cripple Creek Phonolite), under conditions of low w/r, gold solubility would be decreased, relative to zones of higher w/r.

Focussing of fluids into specific channels or pathways through the host rocks – i.e. faults and fractures – produces a zone of higher flux, and thus higher w/r values. Accordingly, the system shifts from right to left on Fig. 2 in zones of focussed fluid flow. This is a potential mechanism for lowering pH and saturating fluids in components that are in solution at the lower w/r and higher pH conditions, including quartz, gold and tellurium. We suggest that focussed fluid fluxes into smaller volumes of host rock in alkaline systems can produce quartz-bearing Au-Te veins. We regard this mechanism of gold precipitation as complimentary to other described triggers, e.g. boiling and cooling (Cooke and Simmons, 2000; and references therein). The association of quartz-bearing alteration (in an otherwise quartz-poor deposit; Jensen and Barton, 2000) with high Au-Te grades is consistent with descriptions of Cripple Creek where high grade Au-(Ag)-Te mineralisation is found in vuggy quartz veins (Kelley et al., 1998). These veins radiate through and out from the alkaline complex, and highest Au grades are found where veins cut that cut crystalline Precambrian (silica-rich granite, gneiss, schist, diorite, and monzonite) and Tertiary (lamprophyre, tephriphonolite, phonotephrite, phonolite and trachyandesite) rocks (Kelley et al., 1998). Low grade disseminated ore (native Au and Au-in-pyrite) is found in higher porosity lithologies of the alkaline complex (Kelley et al., 1998). The evolution of fluids from high pH to lower pH where flow is focussed is also described from the syenite-hosted, intrusion-related Dongping Au-Te-Bi deposit. Gao et al. (2017) modelled initially high pH of fluids ( $> 7$  at 325 °C) responsible for widespread potassic alteration followed by a main stage of mineralisation at  $\text{pH} \sim 5.9$  in silicified zones/veins.

### 5.4. High pH in hydrothermal fluids

The model results in this study demonstrate that silica-undersaturated host rocks can buffer hydrothermal fluids to higher pH. High pH fluids are infrequently recognised in shallow magmatic-hydrothermal and geothermal systems, largely due to the abundance of silica and silica-saturated lithologies in the crust. A notable exception is the presence of highly basic ( $\text{pH} > 12$ ) fluids in ultramafic host rocks (Neal and Stanger, 1984). However, ultramafic lithologies are not typical hosts for epithermal Au-Ag deposits. In the calc-alkaline, silica-saturated rocks that more commonly host epithermal mineralisation, high pH fluids are rare due to the pH buffering reactions that involve quartz. A common mechanism that can increase pH above the “propylitic pH” is dilution (Reed, 1997) (Fig. 5).

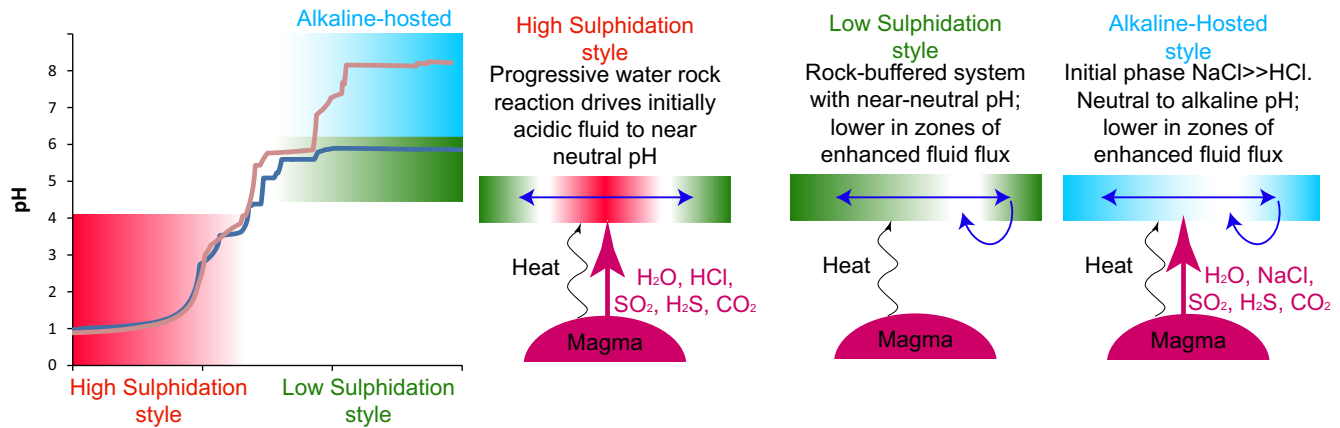


**Fig. 5.** Summary of relationship between pH and water/rock ratio, and the three subsequent styles of epithermal deposit. High sulphidation systems have a significant magmatic volatile input, and typical alteration shows zonation from high w/r advanced argillic and vuggy silica to low w/r propylitic assemblages (Arribas, 1995). Low sulphidation deposits have zonation from moderate w/r argillic alteration to low w/r propylitic assemblages (Hedenquist et al. 2000); evidence for direct input of magmatic volatiles may be equivocal. Alkaline-associated systems show similar alteration and implied w/r to low sulphidation systems (albeit with less silicification and massive quartz veins), but have a stronger signature of magmatic input (Jensen and Barton, 2000). The paucity of advanced argillic alteration in such systems suggests that the magmatic volatile input has NaCl  $\gg$  HCl (Webster et al., 2014).

**Table 3**  
Modelled fluids and natural hot spring discharges from Savo, Solomon Islands and Waramung, Ambitle, PNG. 300 °C compositions are end compositions (minimum w/r) from models; these are modelled in a second stage as cooling to 100 °C with no further host rock reaction. N/A = not applicable, N/M = not measured.

Log w/r	Average Andesite modelled		Cripple Creek modelled		Luise Phonolite modelled		Savo Trachyte modelled		Savo Spring	Waramung Spring
	-1	-1	-1	-1	-1	-1	-1	-1	N/A	N/A
T°C	300	100	300	100	300	100	300	100	100	98
pH	5.85	7.91	8.2	10.2	7.58	8.46	6.07	7.11	7.7	8.8
Cl <sup>-</sup>	0.46	0.46	0.40	0.40	0.40	0.40	0.46	0.41	1.2 × 10 <sup>-4</sup>	0.34
SO <sub>4</sub> <sup>2-</sup>	3.6 × 10 <sup>-4</sup>	1.0 × 10 <sup>-2</sup>	0.20	0.20	0.16	0.16	6.4 × 10 <sup>-4</sup>	0.24	7.1 × 10 <sup>-3</sup>	6.6 × 10 <sup>-2</sup>
HCO <sub>3</sub> <sup>-</sup>	7.2 × 10 <sup>-2</sup>	1.1 × 10 <sup>-5</sup>	2.6 × 10 <sup>-2</sup>	5.8 × 10 <sup>-2</sup>	2.4 × 10 <sup>-2</sup>	3.7 × 10 <sup>-4</sup>	5.7 × 10 <sup>-2</sup>	3.1 × 10 <sup>-2</sup>	1.5 × 10 <sup>-3</sup>	9.2 × 10 <sup>-3</sup>
HS <sup>-</sup>	1.5 × 10 <sup>-3</sup>	4.3 × 10 <sup>-10</sup>	1.3 × 10 <sup>-4</sup>	1.5 × 10 <sup>-3</sup>	1.8 × 10 <sup>-6</sup>	7.8 × 10 <sup>-12</sup>	1.9 × 10 <sup>-3</sup>	4.5 × 10 <sup>-9</sup>	N/M	N/M
SiO <sub>2</sub> (aq)	7.2 × 10 <sup>-3</sup>	1.4 × 10 <sup>-4</sup>	1.5 × 10 <sup>-3</sup>	1.0 × 10 <sup>-2</sup>	2.0 × 10 <sup>-3</sup>	7.6 × 10 <sup>-4</sup>	8.5 × 10 <sup>-3</sup>	8.1 × 10 <sup>-4</sup>	4.3 × 10 <sup>-6</sup>	3.0 × 10 <sup>-3</sup>
Al <sup>3+</sup>	7.9 × 10 <sup>-6</sup>	3.1 × 10 <sup>-8</sup>	2.1 × 10 <sup>-3</sup>	7.0 × 10 <sup>-5</sup>	6.6 × 10 <sup>-4</sup>	1.3 × 10 <sup>-6</sup>	9.2 × 10 <sup>-6</sup>	8.1 × 10 <sup>-8</sup>	1.3 × 10 <sup>-6</sup>	2.1 × 10 <sup>-5</sup>
Ca <sup>2+</sup>	7.7 × 10 <sup>-3</sup>	5.6 × 10 <sup>-3</sup>	4.2 × 10 <sup>-6</sup>	5.6 × 10 <sup>-6</sup>	2.5 × 10 <sup>-5</sup>	8.9 × 10 <sup>-4</sup>	4.5 × 10 <sup>-3</sup>	3.9 × 10 <sup>-4</sup>	6.2 × 10 <sup>-3</sup>	2.0 × 10 <sup>-4</sup>
Mg <sup>2+</sup>	4.7 × 10 <sup>-6</sup>	2.9 × 10 <sup>-7</sup>	2.1 × 10 <sup>-9</sup>	7.5 × 10 <sup>-11</sup>	1.6 × 10 <sup>-8</sup>	1.1 × 10 <sup>-7</sup>	2.2 × 10 <sup>-6</sup>	3.1 × 10 <sup>-5</sup>	5.3 × 10 <sup>-4</sup>	4.0 × 10 <sup>-5</sup>
Fe <sup>2+</sup>	2.4 × 10 <sup>-7</sup>	6.6 × 10 <sup>-10</sup>	7.9 × 10 <sup>-7</sup>	2.5 × 10 <sup>-8</sup>	1.9 × 10 <sup>-7</sup>	7.1 × 10 <sup>-10</sup>	1.0 × 10 <sup>-7</sup>	1.1 × 10 <sup>-7</sup>	7.8 × 10 <sup>-7</sup>	4.0 × 10 <sup>-7</sup>
K <sup>+</sup>	2.9 × 10 <sup>-2</sup>	2.5 × 10 <sup>-3</sup>	9.8 × 10 <sup>-2</sup>	6.6 × 10 <sup>-3</sup>	8.5 × 10 <sup>-2</sup>	5.2 × 10 <sup>-3</sup>	3.0 × 10 <sup>-2</sup>	6.8 × 10 <sup>-3</sup>	4.3 × 10 <sup>-4</sup>	3.6 × 10 <sup>-2</sup>
Na <sup>+</sup>	0.40	0.47	0.73	0.93	0.64	0.71	0.41	0.91	3.6 × 10 <sup>-3</sup>	0.42
Mn <sup>2+</sup>	7.5 × 10 <sup>-3</sup>	3.9 × 10 <sup>-5</sup>	2.3 × 10 <sup>-6</sup>	2.9 × 10 <sup>-6</sup>	1.1 × 10 <sup>-5</sup>	4.9 × 10 <sup>-6</sup>	5.6 × 10 <sup>-3</sup>	3.6 × 10 <sup>-5</sup>	1.5 × 10 <sup>-5</sup>	4.0 × 10 <sup>-8</sup>
Ref									Smith et al. (2010)	Pichler et al. (1999)

The role of dilution in the formation of ore deposits is unclear – whilst the mechanism can increase fluid pH and thus Au and Te solubility, the dilution will lower the concentration of those elements already in solution. In addition, as a diluent travels through a hydrothermal system, it will become less effective as a diluent: the greater the distance that a potential diluent travels, the greater the extent of reaction it will have with the host rocks. The diluent will equilibrate with the host rocks at a progressively decreasing w/r, and an increasing temperature, then they will become increasingly similar in composition to the low w/r hydrothermal fluids, and be unable to act as a diluent.

Smith et al. (2010, 2011) showed that high pH (~8 at 100 °C) hot springs at Savo, Solomon Islands (Table 3) were a consequence of the addition of a diluent (cold meteoric-derived water) to a rock-buffered hydrothermal fluid. The hydrothermal system at Savo is hosted in silica-saturated, mildly alkaline (sodic) intermediate igneous rocks (Smith et al., 2009); the model results in this study show that a rock-buffered fluid would not have high pH in the absence of dilution. The chemistry of the springs show criteria of fluid mixing, disequilibrium and dilution; notably in high Mg<sup>2+</sup>, low Cl<sup>-</sup>, and anhydrite saturation (Smith et al., 2010).

The active hydrothermal system of the Ambitle caldera (Feni Islands group, Bismarck Archipelago, Papua New Guinea) is hosted in silica-undersaturated tephrites, phonolites and trachytes (Wallace et al., 1983). The subaerial Waramung hot springs in the Ambitle caldera discharge fluids at pH 8–9 at ~100 °C (Wallace et al., 1983; Pichler et al., 1999; Meyer-Dombard and Amend, 2014). In contrast to the alkaline springs of Savo, the Waramung springs (Table 3) lack the diagnostic markers of dilution (low Cl<sup>-</sup>, higher Mg<sup>2+</sup> than expected at equilibrium). Thus, it is possible to discriminate the origin of high pH fluids in active hydrothermal systems into diluted or rock-buffered types. The springs at Waramung represent lower temperature discharges of the high pH fluids modelled in this study, and are a natural analogue to the modelled compositions presented herein.

## 6. Conclusions

Epithermal Au mineralisation is typically hosted in sub-alkaline, calc-alkaline lithologies. In these host rocks, fluids may range from highly acidic to near-neutral. Mineral buffering limits the maximum pH to near-neutrality however; alkaline pH requires more

specialised scenarios. One environment in which fluid pH may be basic at high temperature 300 °C is when the host lithology is silica-undersaturated and alkaline. In these compositions, mineral buffers dependent on the presence of quartz are exhausted, allowing for much higher pH.

Silica-undersaturated, alkaline lithologies have been identified as hosts to distinctive epithermal deposits. Alkaline-associated deposits include some of the largest known within the epithermal classification. They have also been recognised for their association with anomalous Te enrichments, relatively silica-poor alteration and magmatic contributions but limited high sulphidation-style alteration and mineralisation. Silica-poor alteration and tellurium enrichment are consistent with water-rock reaction with silica-undersaturated host rocks; however, the paucity of alteration and mineralisation related to highly acidic fluids point towards a distinct primary magmatic fluid (volatile) phase, potentially with a greater preponderance of NaCl over HCl.

### Acknowledgements

This research was funded by the Natural Environment Research Council (UK) grants NE/L002191/1 and NE/M010848/1 in the Security of Supply of Minerals programme. Naden publishes with the permission of the Executive Director, British Geological Survey (NERC). The authors would like to thank Prof. Mark Reed and Dr Jim Palandri for support and feedback.

### Appendix A. Supplementary data

Supplementary data associated with this article can be found, in the online version, at <http://dx.doi.org/10.1016/j.oregeorev.2017.06.028>.

### References

- Arribas, A., 1995. Characteristics of high sulfidation epithermal deposits, and their relation to magmatic fluid. In: J.F.H. Thompson (Editor), *Magma, Fluids, Ore Deposits*. Mineralogical Association of Canada Short Course Series, pp. 419–454.
- Carman, G.D., 2003. Geology, mineralization and hydrothermal evolution of the Ladolam gold deposit, Lihir Island, Papua New Guinea. In: Simmons, S.F., Graham, I. (Eds.), *Volcanic, Geothermal and Ore-Forming Fluids: Rulers and Witnesses of Processes Within the Earth*. Society of Economic Geologists, Littleton, Colorado.
- Cooke, D.R., Simmons, S.F., 2000. Characteristics and genesis of epithermal gold deposits. In: Hagemann, S.G., Brown, P.E. (Eds.), *Gold in 2000*. Society of Economic Geologists, Littleton, Colorado.
- Du Bray, E.A., 2014. Geochemical and modal data for igneous rocks associated with epithermal mineral deposits. 2327–638X.
- du Bray, E.A., 2017. Geochemical characteristics of igneous rocks associated with epithermal mineral deposits—a review. *Ore Geol. Rev.* 80, 767–783.
- Gao, S., Xu, H., Li, S., Santosh, M., Zhang, D., Yang, L., Quan, S., 2017. Hydrothermal alteration and ore-forming fluids associated with gold-tellurium mineralization in the Dongping gold deposit, China. *Ore Geol. Rev.* 80, 166–184.
- Giggenbach, W.F., 1997. The origin and evolution of fluids in magmatic-hydrothermal systems. In: H.L. Barnes (Editor), *Geochemistry of Hydrothermal Ore Deposits*, 3rd Edition. John Wiley and Sons, pp. 737–796.
- Grundler, P.V., Brugger, J., Etschmann, B.E., Helm, L., Liu, W., Spry, P.G., Tian, Y., Testemale, D., Pring, A., 2013. Speciation of aqueous tellurium(IV) in hydrothermal solutions and vapors, and the role of oxidized tellurium species in Te transport and gold deposition. *Geochim. Cosmochim. Acta* 120, 298–325.
- Hedenquist, J.W., Arribas, A.R., Gonzalez-Urien, E., 2000. Exploration for epithermal gold deposits. In: S.G. Hagemann and P.E. Brown (Editors), *Gold in 2000*. Reviews in Economic Geology. Society of Economic Geologists, Littleton, Colorado, pp. 245–277.
- Holland, T.J.B., Powell, R., 1998. An internally consistent thermodynamic data set for phases of petrological interest. *J. Metamorph. Geol.* 16, 309–343.
- Irvine, T.N., Baragar, W.R.A., 1971. A guide to the chemical classification of the common volcanic rocks. *Can. J. Earth Sci.* 8, 523–548.
- Jensen, E.P., Barton, M.D., 2000. Gold deposits related to alkaline magmatism. In: Hagemann, S.G., Brown, P.E. (Eds.), *Gold in 2000*. Society of Economic Geologists, Littleton, Colorado.
- Jensen, E.P., Barton, M.D., 2008. Geology, petrochemistry, and time-space evolution of the Cripple Creek district, Colorado. *GSA Field Guides* 10, 63–78.
- Johnson, J.W., Oelkers, E.H., Helgeson, H.C., 1992. Supcrt92 – a software package for calculating the standard molal thermodynamic properties of minerals, gases, aqueous species, and reactions from 1 bar to 5000 bar and 0 °C to 1000 °C. *Comput. Geosci.* 18, 899–947.
- Kelley, K.D., Romberger, S.B., Beaty, D.W., Pontius, J.A., Snee, L.W., Stein, H.J., Thompson, T.B., 1998. Geochemical and geochronological constraints on the genesis of Au-Te deposits at Cripple Creek, Colorado. *Econ. Geol.* 93, 981–1012.
- Kelley, K.D., Spry, P.G., 2016. Critical elements in alkaline igneous rock-related epithermal gold deposits. In: Verplanck, P.L., Hitzman, M.W. (Eds.), *Reviews in Economic Geology*. Society of Economic Geologists, Littleton, CO.
- Le Maitre, R.W., Bateman, P., Dudek, A., Keller, J., Lameyre, J., Le Bas, M.J., Sabine, P. A., Schmid, R., Sorensen, H., Streckeisen, A., Woolley, A.R., Zanettin, B., 1989. *A Classification of Igneous Rocks and \*\* of Terms: Recommendations of the International Union of Geological Sciences Subcommittee on the Systematics of Igneous Rocks*. Blackwell Scientific, Oxford.
- McPhail, D.C., 1995. Thermodynamic properties of aqueous tellurium species between 25 °C and 350 °C. *Geochim. Cosmochim. Acta* 59, 851–866.
- Meyer-Dombard, D.A.R., Amend, J.P., 2014. Geochemistry and microbial ecology in alkaline hot springs of Ambitle Island, Papua New Guinea. *Extremophiles* 18, 763–778.
- Müller, D., 2002. Gold-copper mineralization in alkaline rocks. *Mineral. Depos.* 37, 1–3.
- Müller, D., Franz, L., Herzig, P.M., Hunt, S., 2001. Potassic igneous rocks from the vicinity of epithermal gold mineralization, Lihir Island, Papua New Guinea. *Lithos* 57, 163–186.
- Neal, C., Stanger, G., 1984. Calcium and magnesium hydroxide precipitation from alkaline groundwaters in Oman, and their significance to the process of serpentinization. *Mineral. Mag.* 48, 237–241.
- Pichler, T., Veizer, J., Hall, G.E.M., 1999. The chemical composition of shallow-water hydrothermal fluids in Tutum Bay, Ambitle Island, Papua New Guinea and their effect on ambient seawater. *Mar. Chem.* 64, 229–252.
- Reed, M., Palandri, J., 2013. SOLTHERM.H08: A database of equilibrium constants for minerals and aqueous species. University of Oregon, Eugene, OR.
- Reed, M.H., 1982. Calculation of multicomponent chemical equilibria and reaction processes in systems involving minerals, gases and an aqueous phase. *Geochim. Cosmochim. Acta* 46, 513–528.
- Reed, M.H., 1997. Hydrothermal alteration and its relationship to ore fluid composition. In: Barnes, H.L. (Ed.), *Geochemistry of Hydrothermal Ore Deposits*. 3rd ed. John Wiley and Sons.
- Reed, M.H., 1998. Calculation of simultaneous chemical equilibria in aqueous-mineral-gas systems and its application to modeling hydrothermal processes. In: Richards, J., Larson, P. (Eds.), *Techniques in Hydrothermal Ore Deposits*. Society of Economic Geologists.
- Richards, J.P., 1990. Petrology and geochemistry of alkalic intrusives at the Porgera gold deposit, Papua New Guinea. *J. Geochem. Explor.* 35, 141–199.
- Richards, J.P., 1995. Alkalic-type epithermal gold deposits – a review. In: Thompson, J.F.H. (Ed.), *Magma, Fluids, Ore Deposits*.
- Richards, J.P., Kerrich, R., 1993. The Porgera gold mine, Papua New Guinea – magmatic hydrothermal to epithermal evolution of an alkalic-type precious-metal deposit. *Econ. Geol.* 88, 1017–1052.
- Shock, E.L., 2007. An updated and augmented version (slop07.dat) of the original SUPCRT92 database (sprons92.dat).
- Sillitoe, R.H., 2002. Some metallogenic features of gold and copper deposits related to alkaline rocks and consequences for exploration. *Mineral. Depos.* 37, 4–13.
- Sillitoe, R.H., 2010. Porphyry copper systems. *Economic Geology*, 106(1): 3–41.
- Simmons, S.F., Brown, K.L., 2006. Gold in magmatic hydrothermal solutions and the rapid formation of a giant ore deposit. *Science* 314, 288–291.
- Simmons, S.F., White, N.C., John, D.A., 2005. Geological characteristics of epithermal precious and base metal deposits, *Economic Geology* 100th Anniversary Volume. Society of Economic Geologists.
- Smith, D.J., Jenkin, G.R.T., Naden, J., Boyce, A.J., Petterson, M.G., Toba, T., Darling, W. G., Taylor, H., Millar, I.L., 2010. Anomalous alkaline sulphate fluids produced in a magmatic hydrothermal system – Savo, Solomon Islands. *Chem. Geol.* 275, 35–49.
- Smith, D.J., Jenkin, G.R.T., Petterson, M.G., Naden, J., Fielder, S., Toba, T., Chenery, S.R. N., 2011. Unusual mixed silica-carbonate deposits from magmatic-hydrothermal hot springs, Savo, Solomon Islands. *J. Geol. Soc.* 168, 1297–1310.
- Smith, D.J., Petterson, M.G., Saunders, A.D., Millar, I.L., Jenkin, G.R.T., Toba, T., Naden, J., Cook, J.M., 2009. The petrogenesis of sodic island arc magmas at Savo volcano, Solomon Islands. *Contrib. Mineral. Petrol.* 158, 785–801.
- Stefánsson, A., Seward, T.M., 2004. Gold(I) complexing in aqueous sulphide solutions to 500 °C at 500 bar. *Geochimica et Cosmochimica Acta* 68(20), 4121–4143.
- Symonds, R.B., Rose, W.I., Gerlach, T.M., Briggs, P.H., Harmon, R.S., 1990. Evaluation of gases, condensates, and SO<sub>2</sub> emissions from Augustine volcano, Alaska: the degassing of a Cl-rich volcanic system. *Bull. Volcanol.* 52, 355–374.
- Wallace, D., Johnson, R., Chappell, B., 1983. Cainozoic volcanism of the Tabar, Lihir, Tanga, and Feni Islands, Papua New Guinea: geology whole-rock analyses, and rockforming mineral compositions. *Austral. gov. publ. service Canberra*.
- Webster, J.D., Goldoff, B., Sintoni, M.F., Shimizu, N., De Vivo, B., 2014. C-O-H-Cl-S-F volatile solubilities, partitioning, and mixing in phonolitic-trachytic melts and aqueous-carbonic vapor ± saline liquid at 200 MPa. *J. Petrol.* 55, 2217–2247.